Electronic Journal of Structural Engineering

Original Article

Cite this: DOI:10.56748/ejse.24552

Received Date:14 November 2023
Accepted Date:19 February 2024

1443-9255
https://ejsei.com/ejse

Response characteristics of surrounding rock and segment structure of large longitudinal slope tunnel

Yang Guanfei[a], Hu haoran[b], Huang xiaolong[a], Luo hu[a], Si gang[a], Chen Yuhua[b], Qiu Junling*[b]

[a] CCCC Second Public Bureau Fourth Engineering Co., Ltd, Luoyang, Henan 471000,China
[b] Chang'an University Highway School of Highway, Shaanxi Xi'an 710064,China
*Corresponding author: junlinggiu@chd.edu.cn

Abstract

To provide reference and guidance for ensuring the safe construction of tunnel construction, taking a mountain road tunnel project as the background, the finite element numerical simulation method is used to study the excavation of large longitudinal slope tunnel by TBM method. The vertical displacement of surrounding rock shows the deformation trend of vault subsidence and arch bottom uplift, and the peak value of lateral displacement decreases gradually with the increase of longitudinal slope gradient. The segment at the vault and arch bottom of the tunnel are subjected to positive bending moment, and the spandrel arch waist and arch foot are subjected to negative bending moment. The maximum value of the absolute value of the axial force is located at the arch waist. In addition, the deformation characteristics of the surrounding rock and the stress characteristics of the segment during the tunnel crossing the fault fracture zone are analyzed. The research shows that the vertical displacement of the surrounding rock is significantly larger than that of the intact stratum, and the closer to the fault fracture zone, the larger the vertical deformation is, and the closer to the tunnel entrance section, the larger the uplift deformation is. The horizontal displacement of the surrounding rock is obviously smaller before it enters the fault fracture zone, and the displacement increases rapidly when it is constructed to the fault range and reaches the peak at the center of the fault. After crossing the fault, the displacement changes little.

Keywords

Tunnel engineering, TBM construction method, Large longitudinal slope tunnel, Numerical simulation, Fracture zone

1. Introduction

With the rapid development of China's transportation industry, more and more tunnels will inevitably cross the complex terrain, so the construction of railroads have to turn to the southwest and other remote mountainous areas (Fan et al,2012). The complex and poor geological conditions of remote mountainous areas in southwest China make the construction of railroad tunnels face great difficulties(He et al,2018;Zhou et al,2014),and geologic disasters such as karst, large deformation of soft rock and rock explosion occur frequently(Chen et al,2015;Fen et al,2022;Jia et al,2021;Yu et al,2018),and TBM tunneling construction is widely used in the construction of railway tunnels in mountainous areas because of its significant advantages such as small construction disturbance, high degree of assembly and mechanization, and long single footage.

Tunnel in the construction process will have a significant impact on a certain range of rock body, the surrounding rock structure stability state is damaged. Scholars at home and abroad have carried out a series of studies around such problems. Aiming at the characteristics of alternating soft and hard changes of the rock body at the palm face of the full-section tunnel boring machine (TBM)in the excavation process, Shi et al. (2020) used model test and numerical simulation methods to explore the dynamic response law of the tunnel surrounding rock in the process of the TBM excavation in the composite stratum. Jiang (2017) took the rock explosion disaster in tunnel TBM construction as the research background, and used a combination of laboratory tests, theoretical analysis, and numerical simulation to discuss the formation and evolution mechanism, control principle and technology of rock explosion in deep composite stratum tunnel TBM construction. Tang (2016) analyzed the key technical problems affecting the stability of the surrounding rock of TBM tunneling in hard rock tunneling in deep coal strata in view of the large depth of the tunnel, the complex distribution of the ground stress field, the uneven development of joints, and the fast speed of digging. Cheng et al. (2016) established a complete TBM model by using FLAC3D and researched the following conditions in the composite strata on the deformation of the surrounding rock, the contact force and friction resistance of the shields during the digging of the TBM. And they used FLAC3D to establish a complete TBM model to study the effects of the following conditions on the deformation of the surrounding rock, shield, and friction resistance during TBM tunneling, and then explored the interaction mechanism between the double shield TBM and the surrounding rock in the composite stratum. TBM tunneling in the construction of large longitudinal slopes faces great risks and challenges, and the construction of the tunneling difficulty is increased, and the jacking force is too large to cause the peripheral rock over-excavation phenomenon in front of the palisade, which can lead to palm face destabilization in serious cases, especially in the construction of the fault fracture zone. The finite element theory is used to simulate the mechanical properties and characteristics of the segment during the construction of the subway shield. The mechanical properties of the segment considering the interaction between the tunnel segment and the stratum are analyzed, which provides an important reference for the design of shield tunnels in different strata(Hou et al.,2018;wang et al.,2021;ye et al.,2011).Based on the actual project, through monitoring and analysis, the main causes of segment cracks, dislocations and other diseases in the construction stage and the weak parts of stress are obtained, which provides a basis for the diagnosis and treatment of segment cracks in shield tunnels and the study of the internal mechanism. It has important reference significance for the calculation design and on-site construction of shield tunnels(Lai et al.,2015;su et al.,2020).

TBM jamming phenomenon often occurs, so to explore the large longitudinal slopes of TBM tunneling peripheral rock and segment structural response characteristics of the environmentally sensitive areas of the railroad tunnel construction is an urgent need to solve the engineering problems.

2. Project Overview

A mountain tunnel passes through a nature reserve and is a typical construction case in an environmentally sensitive area. Therefore, it has the characteristics of sensitive environmental protection, complex geological structure, many long tunnels, and large longitudinal slope. The whole test area belongs to the stress concentration area, and high ground stress will be the main engineering geological problem faced by the deep-buried long tunnel, which is easy to cause large deformation of soft rock and other hazards during construction. The T_3zh stratum is mainly composed of soft rock to hard rock and is partially composed of extremely soft rock (carbon SLATE). Under the condition of high ground stress, the soft rock (SLATE, carbon SLATE) may undergo plastic buckling deformation. The T_2z formation is mainly composed of soft to hard rocks and is partially composed of extremely soft rocks (carbonized SLATE), which does not have the objective conditions for large deformation (except fault fracture zone), so large deformation is always ignored. The sections and grades of large deformation predicted are shown in Table 1.

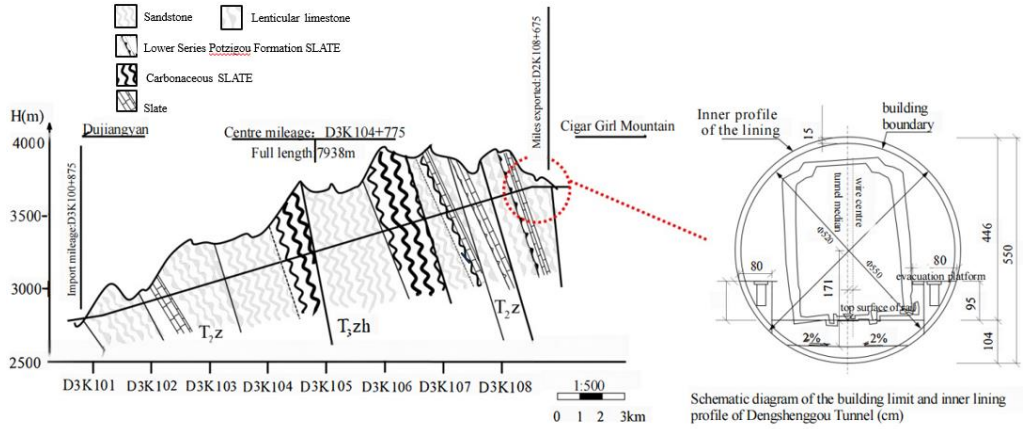

Fig. 1 Overview of construction works

Table 1 Grade prediction of large deformation section of tunnel

Serial number	Mileage	Length	Stratum	Surrounding rock classification	Degree of structural influence	Deformation grade
1	D3K104+400～D3K104+470	70	T_3zh	IV	slight	Level I
2	D3K104+620～D3K104+850	230	T_3zh	IV	slight	Level I
3	D3K105+700～D3K105+900	200	T_3zh	IV	slight	Level I
4	D3K106+100～D3K106+450	350	T_3zh	IV	slight	Level I
5	D3K106+550～D3K106+650	100	T_3zh	IV	slight	Level I
6	D3K106+650～D3K106+750	100	T_2z~T_3zh	V	slight	Level I
7	D3K106+750～D3K106+830	80	T_2z	IV	slight	Level I
8	D3K107+250～D3K107+400	150	T_2z	V	Heavy (fold)	Level I
	Total	1280				

The line length of the tunnel project is about 7938m, and the maximum buried depth is 565m. The longitudinal slope of the line is 65‰/410, 120‰/7200, 0/328. The construction limit is initially proposed to be 5.2m in diameter. Taking into account the need to reserve a certain size, the project design based on the requirements of the tunnel construction boundary, along the radius direction to consider the size of 15cm rich, lining outline is 5.5m diameter of the circle, the effective clearance area above the tunnel rail surface is 19.5m²; The tunnel area is covered with Quaternary Holocene artificial filled gravel soil, landslide accumulated gravel soil, alluvial pebble soil, slope colluvium, gravel soil, slope residual silky clay, and Pleistocene moraine and ice water accumulated gravel soil. The rock formations traversed by the tunnel mainly include five types, namely sandstone and SLATE, metamorphic sandstone plywood and lenticular limestone, Lower Series Botzigou Formation SLATE, sandstone sandwich limestone and fault breccies, as shown in Fig. 1. And the adverse geological disasters along the project can be summarized as high intensity, fault fracture zone development, landslide, rock pile, debris flow, high ground stress, karst, harmful gas, high ground temperature, etc. Special soil is seasonal frozen soil.

The area along the tunnel belongs to the eastern section of Xiaojin arc structural belt overall. Meanwhile, the geological structural belt in the study area extends from east to west. At the same time, the structural belt also includes many linear distributed arc-shaped folds on the south of the arc top, which are coordinated and compact, and the tunnel belongs to a large longitudinal slope tunnel. At the same time, the tunnel is faced with the engineering geological conditions of large, buried depth, high ground stress, fault fracture zone development and lithology mainly soft rock, and the stress of surrounding rock and tunnel lining structure is relatively complicated when TBM is used in the construction of this large longitudinal slope. Therefore, the numerical simulation method is used to carry out multi-condition analysis and comprehensively consider the influence of many factors to study the internal force response characteristics of the surrounding rock and segment of the TBM construction of the medium longitudinal slope tunnel.

3. Construction simulation under complete formation condition

3.1 Model Overview

Through the use of finite element software FLAC 3D for numerical simulation, combined with the actual situation of the project, and based on St.Venant's principle of analysis(Wang et al,2021,Zhen et al,2022),the length of the left and right boundaries is 5 times the hole diameter from the edge of the hole, the lower boundary is 5 times the hole diameter from the edge of the tunnel hole, and the upper boundary is 23m from the edge of the tunnel hole. Therefore, the size of the model is: length×width×height = 46m×40m×60m.The overall model calculation is shown in Fig. 2.

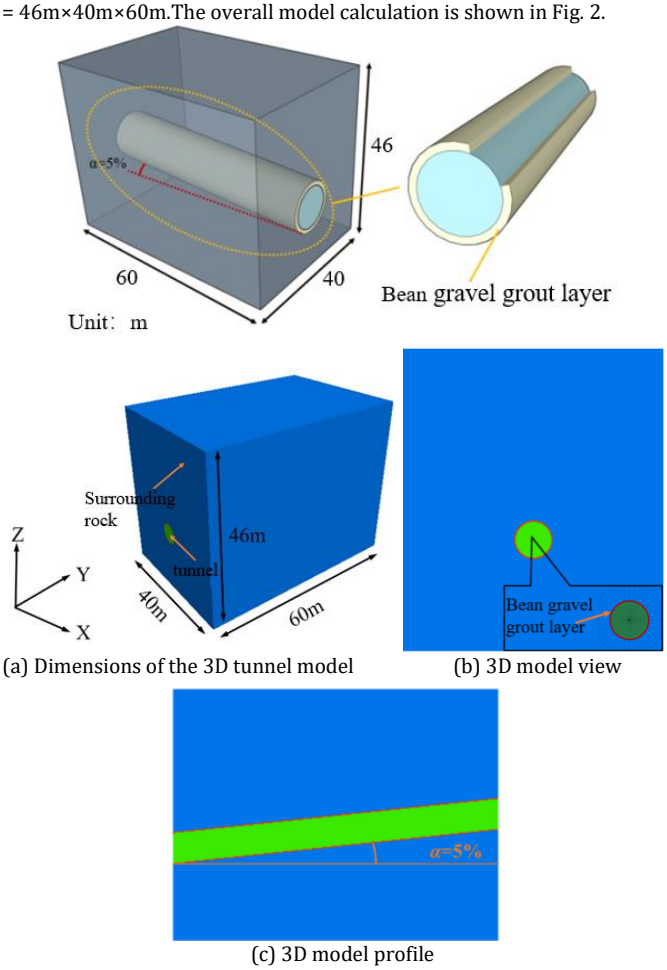

(a) Dimensions of the 3D tunnel model (b) 3D model view

(c) 3D model profile

Fig. 2 Schematic diagram of calculation model

In the numerical modeling, the mechanical parameters of grade IV surrounding rock are selected according to the indoor test results, and the supporting parameters of segment lining are shown in Table 2. Since the longitudinal segment lining is a prefabricated concrete structure connected by bolts, the strength of the concrete segment lining structure

is reduced by 20% to reflect the weakening effect of bolts. The constraint conditions of the model include: the upper part is the free surface, the horizontal constraint in the X direction is applied to the left and right boundaries, the horizontal constraint in the Y direction is applied to the front and rear interfaces, and the constraint in the vertical direction is applied to the lower part of the model.

Table 2 Parameters of segment support

Material type	densities ρ(g/cm^3)	cohesive force c (MPa)	friction angle φ (°)	Modulus of elasticity E (GPa)	Poisson's ratio μ
On-site rock samples	2.31	0.54	34.2	5.74	0.22
lining segment	2.45	-	-	33.5	0.2
Bean gravel grouting layer	2.68	0.55	33.5	3.8	0.33

3.2 Design of monitoring point

In order to study the deformation response of the surrounding rock and segment under five working conditions, such as longitudinal slope gradient of 5%, 12%, 15%, 20% and 30%, the internal force data of the tunnel segment and various parts of the lining structure(vault, spandrel, hance, arch footing and inverted arch)were extracted, and the arrangement of the measurement points and the design of the working conditions are shown in Fig. 3.

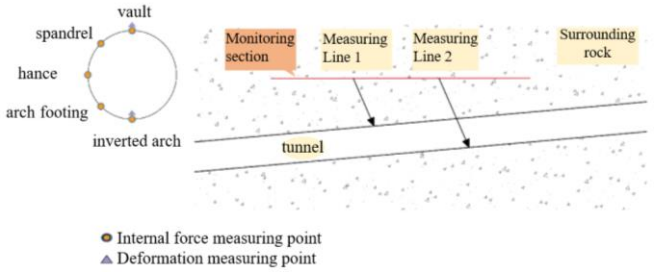

Fig. 3 Measurement point arrangement

3.3 Construction process simulation

Because it is impossible to simulate the rotary rock breaking process of the TBM cutterhead in the software, the corresponding load can only be applied on the cutterhead to simulate the rotary rock breaking process of the disc cutter, and the tunneling pressure acting on the face of the cutterhead is replaced by applying uniform load. Generally, the grouting method of filling bean gravel after segment is adopted. After the segment is activated, the bean gravel layer is activated synchronously, and finally deleting the gravel layer and activating the grouting layer. The steps of adding loads for numerical simulation in construction are as follows:

1. The self-weight stress field reaches equilibrium;
2. The cutterhead applies thrust to the front surrounding rock;
3. The null model is used to eliminate the excavation soil to simulate the TBM construction process;
4. Activate the first ring segment unit and the bean gravel layer;
5. Remove the bean gravel and generate the backfill layer to simulate the changes in the later stage of grouting;
6. Repeat the above steps, and the TBM continues to advance until it advances to Y=60m.

3.4 Model Calculation Analysis

Deformation law of surrounding rock

Through the vertical displacement changes of different tunnel longitudinal slope gradient when the tunnel passes through, it is found that the vertical displacement and deformation direction of the deeply buried circular tunnel after excavation are all along the direction of the center of the tunnel, as shown in Fig. 4, the statistics of different longitudinal slope gradient under the tunnel arch and the bottom of the peripheral rock deformation peaks, it can be seen that with the increase of the longitudinal slope gradient, the peripheral rock subsidence maximum and the peak of the deformation of the rumble is gradually decreasing, but the amount of change is relatively small. This is due to the influence of the TBM weight, the lower part of the arch of a certain range of surrounding rock extrusion, the greater the inclination is the more significant effect of extrusion, so with the increase in slope of the tunnel arch deformation value gradually reduced.

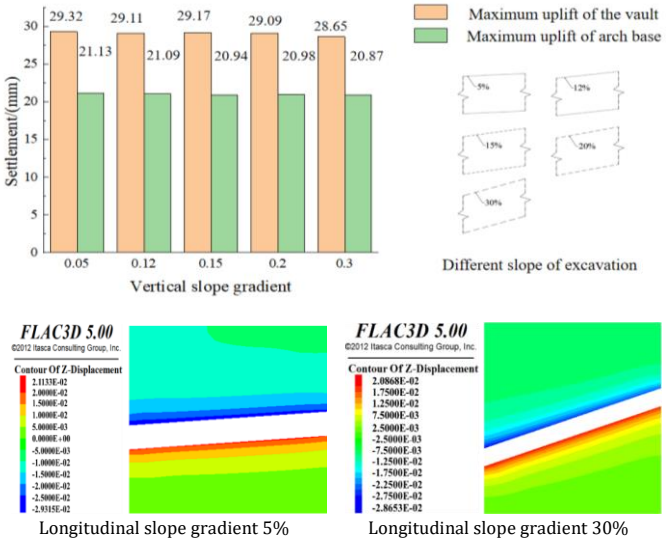

Fig. 4 The change of vertical displacement during tunnel penetration under different longitudinal slope gradients of tunnel

Due to the circular excavation cross-section and the large burial depth of the tunnel, the horizontal convergence deformation of the tunnel is relatively small compared to the vertical deformation. The horizontal displacement changes of the surrounding rock under different longitudinal slope gradients during tunnel penetration were extracted as shown in Fig.5. During TBM excavation, the horizontal displacement shows a trend of convergence towards the inside of the tunnel. As excavation progresses, the horizontal deformation range of the tunnel gradually expands, with the main deformation range concentrated within a certain range of the horizontal direction of the tunnel cross-section; Compared to the construction of the flat slope section, with the longitudinal slope construction, the horizontal deformation of the surrounding rock around the tunnel presents a symmetrical distribution feature along the centerline of the tunnel, and the main deformation range is concentrated within the 45°range above and below the horizontal direction of the tunnel section. As the longitudinal slope gradient increases, the horizontal deformation of the surrounding rock at the arch waist of the tunnel becomes larger as it approaches the edge of the tunnel, and its peak horizontal convergence deformation gradually decreases.

Analysis of internal force of segment structure

The axial force and bending moment data of segment vault, left and right spandrel, left and right hance, left and right arch foot and middle position of inverted arch are shown in Fig. 6. It can be seen that the bending moment change of segment structure presents symmetrical distribution characteristics, and the maximum positive bending moment appears at the top of segment, while the maximum negative bending moment occurs at the haunch of segment. Under different working conditions, the bending moment of segment structure shows that the top and bottom of segment are affected by positive bending moment, while the haunch is affected by negative bending moment. It can be seen from Fig. 6 (a) that with the increase of longitudinal slope, the maximum positive bending moment and the maximum negative bending moment gradually increase.

With the analysis of the distribution characteristics of the bending moment, the axial force distribution data of the segment at different parts of the first ring segment are extracted as shown in Fig. 6 (b). The analysis can be obtained:

I. Under certain longitudinal slope conditions, all the segments are compressed, with the maximum axial force acting on the arch waist, followed by the arch crown and the minimum axial force acting on the arch foot. The axial forces on the arch crown and inverted arch, as well as on the arch shoulder and arch foot are relatively close. Taking a longitudinal slope of 5% as an example, when the tunnel passes through, the axial force on the arch waist is about 14.9% greater than that on the arch crown, and about 49.2% greater than that on the arch foot. Therefore, during construction, it is important to pay attention to the stress state at the position of the segment arch crown and arch bottom.

II. With the increase of longitudinal slope gradient, the maximum axial force of the segment gradually decreases, the longitudinal slope gradient increases from 5% to 30%, the maximum axial force of the segment increases by 7.94%, the empirical calculations do not reach the ultimate strength of reinforced concrete, the segment lining structure is in a safe state.

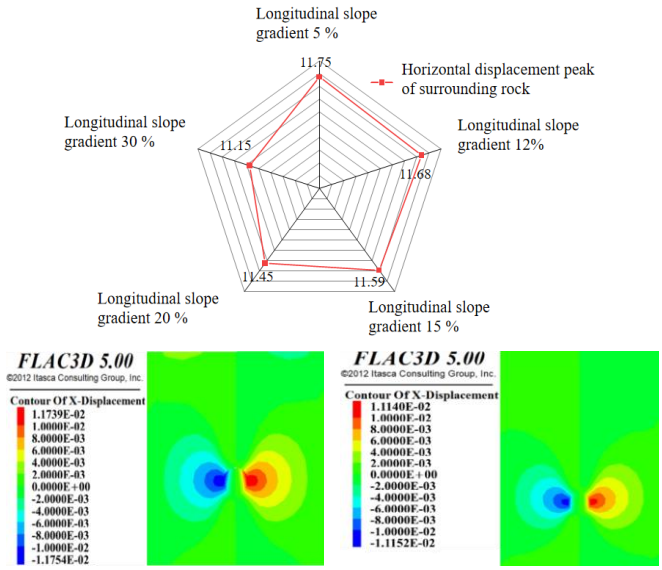

(a)Longitudinal slope gradient 5% (b)Longitudinal slope gradient 30%

Fig. 5 Variation of horizontal displacement of surrounding rock under different longitudinal slope gradients

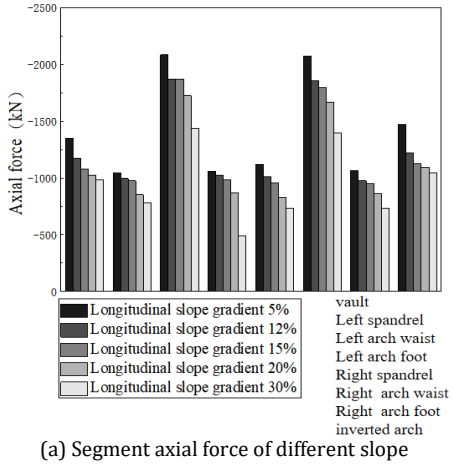

(a) Segment axial force of different slope

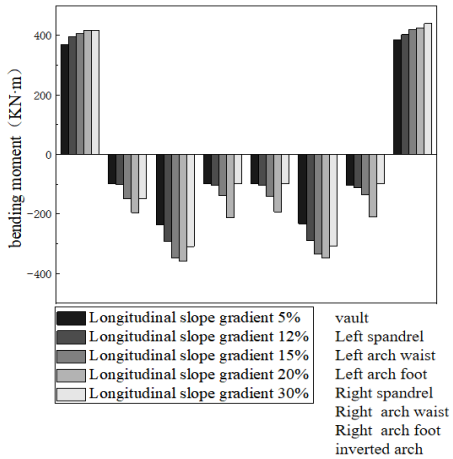

(b) Segment bending moment of different slope

Fig. 6 Axial force and bending moment data of segment

4. Construction simulation under fault fracture zone condition

According to the existing completed engineering cases, there is a risk of jamming when the tunnel passes through the fault fracture zone. In the early field investigation stage of this tunnel project, it is known that the line will cross the fault fracture zone, and the surrounding rock is highly broken. Therefore, it is necessary to study the construction mechanical characteristics of TBM crossing the fault fracture zone. Based on this working condition, this section establishes a mechanical response model of single shield TBM crossing the fault fracture zone and reveals the mechanical response characteristics of surrounding rock and segment structure when crossing the orthogonal fault fracture zone under different longitudinal slope gradients.

4.1 Calculation model

Relying on the tunnel crossing the active fault zone, the thickness of the fault zone is 20m,orthogonal to the tunnel direction and the inclination angle is 80°,15 times the diameter of the tunnel on both sides of the tunnel centerline as the left, right and up and down boundaries of the model, and 100 m in the longitudinal direction, so the model dimensions are: length × width × height=80 m×80 m×100 m. The overall three-dimensional model is shown in Fig. 7 (with the longitudinal slope of 5% as an example). Referring to the studies of (Zhao et al,2021; Sun et al,2020), the fault is simulated by the method of weakening the material parameters and adopting the Moore-Coulomb ontological relationship, and the fault material physical and mechanical parameters are shown in Table 3.

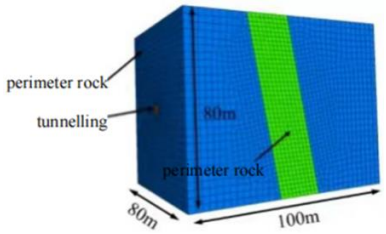

Fig. 7 Schematic of finite element model

4.2 Calculations

Peripheral rock displacement field law

The vault settlement and uplift deformation values under different longitudinal slope gradients are shown in Fig 8. The variation trend of vertical displacement of surrounding rock under different slopes is different from that of excavation in the complete bottom layer. The settlement generated during the penetration mainly comes from the fault fracture zone, and the uplift generated mainly comes from the construction section in front of the fault fracture zone. This is because the fault fracture zone is more affected by TBM tunneling disturbance. In addition, the fault fracture zone has a slip trend along the dip direction; with the increase of the longitudinal slope gradient, the settlement area at the fault fracture zone gradually expands. Compared with the complete stratum, the peak value of the vault settlement and the peak value of the uplift deformation increase significantly, and the closer to the fault fracture zone, the greater the vertical deformation.

After the tunnel is penetrated, a vertical displacement measuring point is arranged at 2m intervals along the tunnel footage to explore the change of vertical displacement of surrounding rock after TBM excavation under longitudinal slope.

Fig.9 gives the vertical deformation and uplift deformation curves of the surrounding rock under different longitudinal slope gradients. It can be seen from Fig.9(a)that the vault settlement gradually increases with the increase of the distance from the fault, but the increment is less. When entering the fault area, the vertical settlement of surrounding rock increases obviously, and the vertical displacement at the center of the fault increases to the maximum. When the monitoring point moves from the center of the fault to the direction away from the fault, it begins to decrease again. When it is outside the influence range of the fault area, it is basically stable at a fixed value. It can be seen from the figure that the larger the longitudinal slope, the smaller the influence range of the fault on the vault settlement.

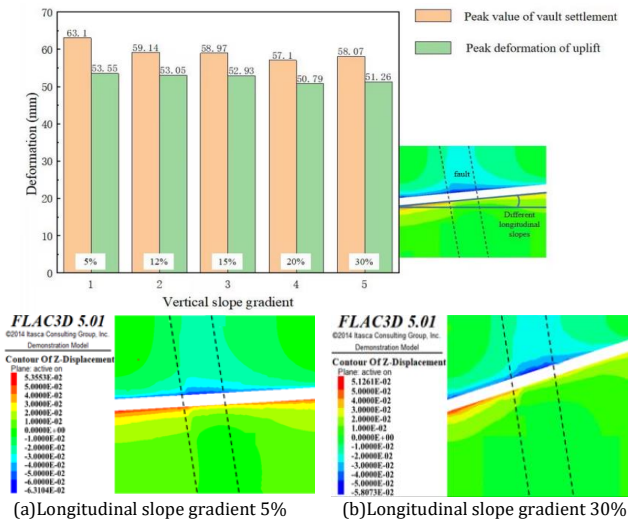

(a)Longitudinal slope gradient 5% (b)Longitudinal slope gradient 30%

Fig. 8 Settlement and bulge deformation values of vault for different longitudinal slope gradients

Table 3 Model parameters

designation	densities ρ (g/m³)	bulk modulus K (MPa)	shear modulus G (MPa)	modulus of elasticity E (GPa)	Poisson's ratio μ	angle of internal friction φ (°)	cohesive force c (kPa)
geologic fault	1.8	1.04×10^3	2.07×10^2	0.5	0.42	22	150

From Fig.9(b), the deformation of the tunnel exit section is larger than that of the entrance section; with the increase of longitudinal slope gradient, the uplift deformation of surrounding rock remains almost unchanged before reaching the fault fracture zone. When the construction reaches the fault fracture zone, the uplift deformation of surrounding rock begins to decrease. When the longitudinal slope is 5% ~ 12%, the uplift deformation of surrounding rock increases gradually when it leaves the influence range of the fault, and then stabilizes near a fixed value when it is within a certain range from the outlet. When the angle is 12% ~ 20%, it tends to be stable after decreasing outside the fault affected area. When the longitudinal slope is greater than 30%, the uplift deformation outside the fault affected area gradually decreases, and the reduction is more obvious in the fault fracture zone, and then stabilizes near a certain value in the fault to the outlet section. Therefore, the larger the longitudinal slope, the more significant the influence of the fault fracture zone on the uplift deformation of the surrounding rock.

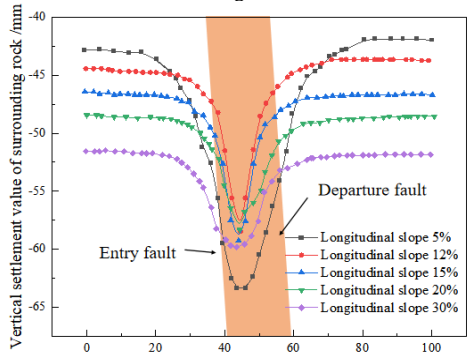

(a)Vertical settlement of the surrounding rock

(b)Deformation of surrounding rock uplift

Fig. 9 Vertical settlement and convergent deformation curves of surrounding rock under different longitudinal slope gradients

For the horizontal displacement of the surrounding rock, because the horizontal displacement variation law of surrounding rock on both sides of the tunnel is relatively consistent, the left arch waist is selected for analysis. Fig. 10 shows the variation law of the horizontal displacement of the left arch waist along the tunnel footage direction under different longitudinal slope gradients. From the diagram, it can be seen that the horizontal displacement of the left arch waist is ' bell-shaped ' distribution. Before entering the fault failure zone, the horizontal displacement did not change significantly. After entering the fault, the displacement suddenly increased and reached the maximum at the center of the fault fracture zone, and then tended to be stable. With the increase of longitudinal slope, the peak value of horizontal displacement in the center of the fault fracture zone gradually decreased and the curve shape remained basically unchanged.

Analysis of internal forces in segment

The tunnel crossing the fault zone is extremely unfavorable to the segment structure, so the distribution of the segment internal force at the fault zone when the tunnel is extracted is shown in Fig.11. Due to the influence of the fault zone excavation disturbance effect, along the fault dip direction to produce slip, so through the orthogonal fault zone construction segment internal force than in the intact rock layer construction is larger, segment axial force basically shows a tendency to be compressed, while the bending moment is manifested as the top and bottom of the compression, the arch girdle parts of the tensile; through the comparison can be seen by the intact ground excavation construction of the segment internal force peaks (absolute value) compared to each other, it can be found that in the fault zone construction in the segment structure stress distribution is shown in Fig. 11. It can be found that the increase of the internal force of the segment is obvious when constructing in the fault broken zone, for example, taking the longitudinal slope of 5% as an example, when the tunnel passes through, compared with the construction in the complete stratum, the peak axial force at the fault broken zone increases by about 52.3%, and the peak bending moment increases by about 13.4%.

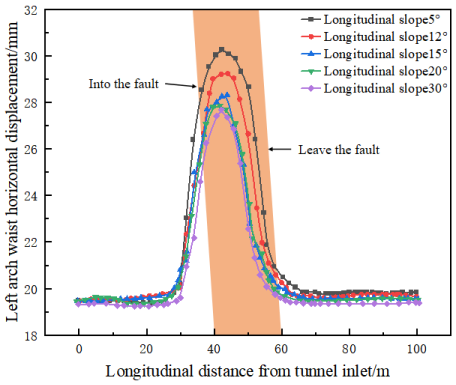

Fig. 10 Horizontal displacement change rule of left arch girdle under different longitudinal slope gradient

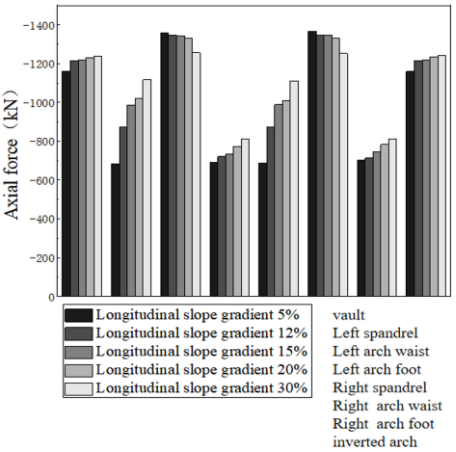

(a)Segment axial force of different slope

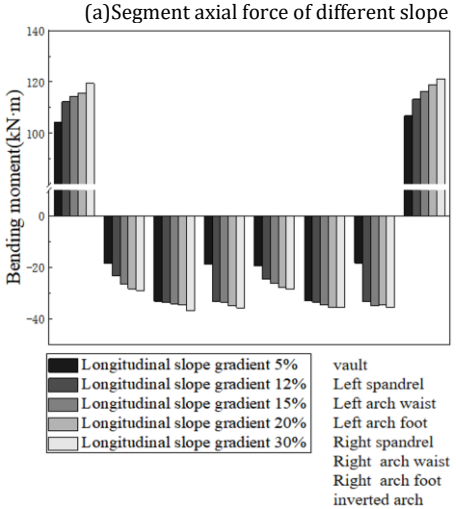

(b)Segment bending moment of different slope

Fig. 11 Axial force and bending moment data of segment across fault fracture zone

5. Conclusion

In this chapter, based on FLAC 3D finite difference simulation software, the fine simulation of single shield, bean gravel and segment are carried out, and the dynamic response model of construction under the condition of large longitudinal slope is established. The deformation of surrounding rock and the distribution of internal force of segment in complete stratum and fault fracture zone stratum under different longitudinal slope of tunnel are compared and analyzed. The main conclusions are as follows:

When construction boring is carried out in complete strata:

I. The vertical displacement of single shield TBM excavation shows the deformation trend of vault subsidence and arch bottom uplift, and the displacement change of surrounding rock shows obvious spatial excavation effect, and the farther away from the tunnel face, the vault settlement and uplift deformation gradually increase; with the increase of longitudinal slope gradient, the peak value of vault settlement and uplift deformation decreases gradually.

II. Horizontal displacement of tunnel surrounding rock is symmetrically distributed along the center line of the tunnel, and the main deformation range is concentrated within 45° above and below the horizontal direction of the tunnel section, and the closer to the edge of the tunnel, the larger the horizontal deformation is, and with the increase of longitudinal slope gradient, the peak horizontal displacement gradually decreases.

III. All the segments are under pressure. For the bending moment distribution of the segment, the vault and arch bottom are subjected to positive bending moment, and the arch shoulder, arch waist and arch foot are subjected to negative bending moment. The maximum value of the absolute value of the axial force is located at the arch waist, and the maximum value of the absolute value of the bending moment is located at the vault. With the increase of the longitudinal slope, the peak value of the absolute value of the axial force of the segment gradually decreases and the peak value of the absolute value of the bending moment gradually increases.

When the fault fracture zone is excavated:

I. With the increase of longitudinal slope gradient, the settlement area at the fault fracture zone gradually expands, and the peak value of vault settlement and uplift deformation increases significantly compared with that in the complete stratum, and the closer to the fault fracture zone, the greater the vertical deformation is, and the closer to the tunnel entrance section, the greater the uplift deformation is.

II. The lateral deformation of surrounding rock converges to the center along the tunnel body, the horizontal displacement is obviously small before entering the fault zone, and the displacement increases rapidly when the construction is within the fault zone and reaches the peak at the center of the fault zone, and the displacement changes are small after crossing the fault, and with the increase of the longitudinal slope gradient, the peak horizontal displacement at the center of the fault zone decreases gradually, and the shape of the curve is basically kept unchanged;

III. The segment is all compressed, while the bending moment is characterized by compression at the top and bottom, and tension at the arch waist. The internal force of the segment increases significantly during construction in the fault fracture zone. Taking the longitudinal slope of 3° as an example, compared with the construction in the complete stratum, the peak bending moment of the axial force at the fault fracture zone increases by about 52.3% and 13.4%.

References

CHEN Weizhong, XIĀO Zhenglong, TIAN Hongming. Research on extrusion large deformation of deeply buried high geostress TBM tunnel and its control technology[J]. Journal of Rock Mechanics and Engineering,2]. Journal): 2215-2226. DOI: 10.13722/j.cnki.jrme.2015.1000

Cheng J L, Yang S Q, Du L K, et al. Three-dimensional numerical simulation on interaction between double-shield TBM and surrounding rock mass in composite ground[J]. Chinese Journal of Rock Mechanics and Engineering, 2016, 35(3): 511-523.DOI:10.13722/j.cnki.jrme.2015.0693

Fan Min, Li Yuanfu. Research on emergency rescue design of high-speed railroad tunnels in difficult and dangerous mountainous areas[J]. Railway Standard]. Railway12(10): 66-68+72. DOI: 10.13238/j.issn.1004-2954.2012.10.029

Feng Huanhuan, Hong Kairong, Yang Yandong, et al. Research and application of key technology of TBM tunnel construction under extremely complex geological conditions[J]. Modern Tunneling Technology, 2022, 59(01): 42-54. DOI: 10.13807/j.cnki.mtt.2022.01.005

Hou Gongyu, Yang Yue, Li Xiaorui et al. TBM tunnel segment longitudinal stress transfer law [J]. Modern tunnel technology,2018 zhongguo kuangye daxue (02): 65-71. The DOI: 10.13807 / j.carol carroll nki determined by MTT.2018.02.009

HE Zhimin, LI Yuanfu, FAN Min. Discussion on safety grade determination of difficult mountainous railroad tunnels based on the superiority evaluation method[J]. Railway Standard Design,2018,62(11): 125-128+160.DOI: 10.13238/j.issn.1004-2954.201801070001

JIA Jianbo, GAO Guangyi, WEN Xingming. Comprehensive management technology of large-scale surge in Gaoligongshan tunnel[J]. Tunnel Construction (in Chinese and E]. Tunnel2021,41(S1): 394-400.

Jiang,B.Y..Research on rock explosion breeding and control mechanism of TBM construction in deep composite ground tunnel [D]. China University of Mining and Technology, 2017.

Lai Jinxing, Qiu Junling, Pan Yunpeng et al. of shield tunnel segment lining cracks in comprehensive monitoring and analysis [J]. Modern tunnel technology, 2015, 52(02): 186-191.The DOI: 10.13807 / j.carol carroll nki determined by MTT.2015.02.028

Lincoln Shi, Hui Zhou, Ming Song, Jingjing Lu, Chuanqing Zhang, Xinjing Lu. experimental study on disturbance modeling of TBM excavation in deep composite strata[J]. Geotechnics,2020,41(06): 1933-1943.DOI: 10.16285/j.rsm.2019.1014.DOI: 10.16285/j.rsm.2019.1014

Sun Lang, Ou Xiangping, Yan Zhihao, et al. Influence of geological characteristics of fault fracture zones on the stability of tunnel surrounding rock[J]. Journal of Wuhan University of Technology,2020,42(03): 23-31.

Su Kai, Zhou Xiaoyang, Yang Fengwei et al. Research on Mechanical characteristics of new parallelogram segment lining structure of TBM tunnel [J]. Journal of Wuhan University (Engineering and Technology Edition), 2020, 53(06): 471-482. DOI:10.14188/ J.1671-8844.2020-06-001

Tang Bin. Research on perimeter rock stability and support technology of deep coal mine tunnel TBM construction[D]. Anhui University of Technology,2016.

Wang Cheng, Tang Peng, Zhuang Haiyang et al. Consider done across large diameter pipe gallery of shield tunnel seismic performance research [J]. Journal of natural disasters, 2021, 30(01): 116-123.The DOI: 10.13577 /j.j nd.2021.0112

WANG Feiyang, ZHOU Kaige, FANG Yong, et al. Analysis of surrounding rock disturbance induced by TBM excavation of deeply buried railroad tunnel[J]. Tunnel Construction (in Chinese and English), 2021, 41(02): 240-247.

Ye Fei, He Chuan, Wang Shimin. During the construction of shield tunnel lining segment mechanical characteristics and its impact analysis [J]. Rock and soil mechanics, 2011, 32(6): 1801-1807 + 1812. DOI: 10.16285 / sm j.r.2011.06.040

Yu Li, Wang Xiaoliang, Wang Mingnian, et al. Research on cooling technology of diversion tunnel for TBM construction[J]. Tunnel Construction (in Chinese and English), 2018, 38(11): 1778-1784.

ZHOU Jianjun, YANG Zhenxing. Discussion on key issues of TBM construction in deep-buried long tunnels[J]. Geotechnical Mechanics,201]. Geotechnical305. DOI: 10.16285/j.rsm. 2014.s2.049

Zhang Heng, Chen Shougen, Tan Xinrong, ZHAO Yubao. Research on mechanical behavior of shield tunnel segments in different strata [J]. Chinese Journal of Underground Space and Enginee]. Chinese5,11(04):845-851.

ZHENG Weiqin, XU Jie, SUN Jie, et al. Force characteristics of TBM tunnel tubes in composite strata[J]. Journal of Shandong University (Engineering Edition), 2022, 1-5.

ZHAO Qingyun. Study on deformation damage and control of peripheral rock in tunnel crossing fault fracture zone[D]. Hefei: Anhui University of Architecture, 2021.